ISSN 1392–1320 MATERIALS SCIENCE (MEDŽIAGOTYRA). Vol. 23, No. 1. 2017

Enhanced Absorption in Organic Thin-Films from Imprinted Concave Nanostructures

Arkadiusz Jarosław GOSZCZAK *, Horst-Günter RUBAHN, Morten MADSEN

NanoSYD, Mads Clausen Institute, University of Southern Denmark, Alsion 2, Sønderborg, DK-6400, Denmark

crossref http://dx.doi.org/10.5755/j01.ms.23.1.14188

Received 18 February 2016; accepted 11 March 2016

In this work, a rapid, replicable method for imprinting concave nanostructures to be used as functional light-trapping nanostructures in organic thin-films is presented. Porous anodic alumina templates were fabricated both by anodization of thick Al foils and by anodization of submicrometer thin Al films evaporated via e-beam evaporation on Si substrates. The template formation leads to natural patterning of the underlying Al layers that are used as rigid masters for stamp fabrication, after selective etching of the porous anodic alumina. PDMS stamps were made after replicating the Al concave patterns and used for imprinting of spin coated photoresist on glass substrates. We have investigated semi-periodic and aperiodic imprinted large concave patterns fabricated from rigid masters after anodization of Al in H_3PO_4. We show that metal covered imprinted concaves show enhancement in absorption that is attributed to field enhancement and diffuse scattering, leading to efficient light trapping for a selected active layer material (P3HT:PCBM).
Keywords: Al concaves, enhanced absorption, imprinting, PAA.

1. INTRODUCTION

Solar devices made from organic materials have gained increasing attention in the past years compared to their inorganic counterparts, due to promising advantages such as transparency, flexibility and ease of processing [1]. Despite the fact that the efficiencies of the organic solar cells have increased to 10.6 % [2], their power conversion efficiencies are still lower than those of their inorganic counterparts that approach efficiencies of more than 20 % [3]. This issue can be addressed by integration of structured electrodes in organic solar cell architectures, which can lead to an enhancement of light absorption and thereby an increase of power conversion efficiency [4 – 6].

At present, efficient light-trapping strategies via nanostructuring can be divided into non-plasmonic related designs and plasmonic related designs [7, 8]. In such designs, employment of features at the nano- and micron-scale that trap light of specific wavelengths can increase the light absorption and charge generation in the active layer, and furthermore improve charge extraction at the electrodes surface. Textured or rough surfaces in the solar device enhance the absorbance by diffuse scattering of light within the active layer [9, 10], periodic gratings are used to diffract light into the active layer in the solar cell [11 – 13], nanoparticles improve either absorption by scattering of incident light, or concentrate the electromagnetic near-field by employing localized surface plasmon resonances [14 – 17].

The application, though, of such techniques to devices with dimensions that exceed those at the laboratory scale, together with faster fabrication methods, is challenging. Imprinting techniques are convenient methods for patterning surfaces at the nanoscale, and they act as an appealing alternative to the expensive tools used in UV-lithography and electron-beam lithography [18, 19]. Organic solar cells can for example be structured by soft imprinting of grating structures using a resist or by direct patterning of interfacial layers, printing of nanodots etc. [20 – 22].

For the majority of the imprinting processes, the time consuming and small scale patterning method of electron beam lithography for the fabrication of rigid masters, which are used for imprinting, is applied. Porous anodic alumina templates (PAA) [23 – 25] have been realized as an alternative method to implement faster imprinting processes and also obtain larger nano-patterned areas in the fabrication of nanostructures [26]. This involves usually the anodization process of high purity Al foils in selected acidic electrolytes to tailor the surface morphology of organic layers [27], imprinting of polymer layers for the formation of ordered pillars [28, 29], or formation of nanovoids for imprinted localized plasmonic structures [30]. In this work, we present a method that uses the underlying concave pattern resulting from the anodization process of Al. Fabrication of such Al concave patterns after anodization of thick Al foils are known in literature and their relation to the formation mechanism of porous alumina film and the operating conditions has been investigated [31 – 33]. Thick Al foils though have a rough surface on the microscale introducing the necessity of additional pre-treatment steps [34, 35].

We anodize untreated thick Al foils as well as thin Al films on supporting surfaces, and compare their resulting imprint patterns. We show that the formation of Al concaves on supported substrates after anodization of submicrometer Al films evaporated on Si results in shorter processing times for the anodization and at the same time avoids the irregularities present on untreated Al foils. The concave patterns are then replicated using PDMS (polydimethylsiloxane) for the fabrication of reusable soft imprinting stamps for imprinting of spin coated photoresist on glass insulating substrates. The imprinted samples are

* Corresponding author. Tel.: +45-6550-1616.
E-mail address: *goszczak@mci.sdu.dk* (A. J. Goszczak)

compatible with metal evaporation techniques and can be used for the formation of nanopatterned electrodes for organic thin films. To demonstrate the effect of the structures on the optical properties we conduct reflectivity measurements on devices consisting of evaporated metal layers on the imprinted concave nanopatterns decorated with a mixture of poly-3-hexyl thiophene (P3HT): phenyl-C_{61}-butyric acid methyl ester (PCBM).

2. EXPERIMENTAL

Fig. 1 shows in brief the process flow to obtain nanoimprinted concaves on photoresist with a schematic representation of the samples in the left column and SEM images of samples made after a series process in the right column. For the fabrication of a rigid master, a thin Al layer is initially anodized in H_3PO_4 under constant voltage and temperature to form a porous template (Fig. 1 a). The formed PAA template is then etched selectively in a H_2CrO_4/H_3PO_4 mixture to expose the underlying Al concave patterns (Fig. 1 b), a process that is typically employed in double step anodization of thick Al foil to induce guided pore formation and better pore arrangement during the second anodization [36, 37]. Following this, a PDMS stamp is fabricated by replicating the rigid master, resulting in an inverse pattern of the Al concave nanostructures (Fig. 1 c). Finally the PDMS stamp can be used multiple times to imprint spin coated resist on quartz samples (Fig. 1 d).

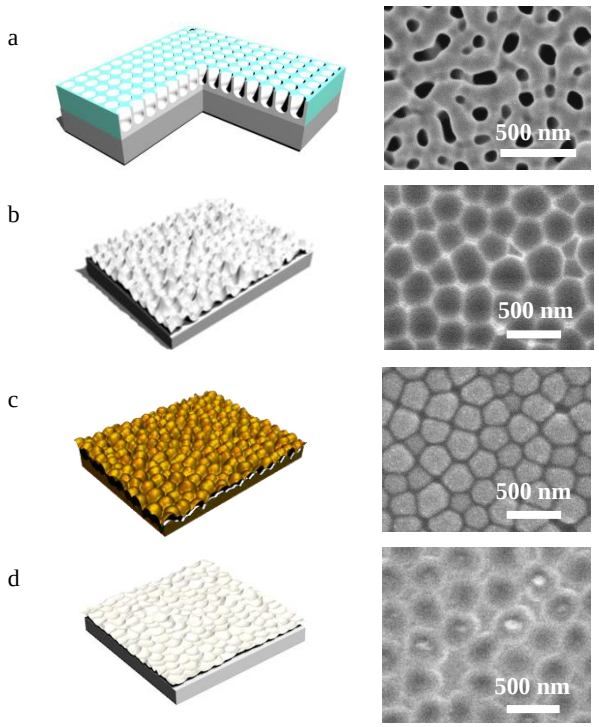

Fig. 1. Schematic overview (in the left column) and SEM images (in the right column) of the samples fabricated at each step of the fabrication line for imprinting structures: a – PAA template from anodization of Al; b – Al dimples after etching PAA in (a); c – PDMS stamp after replication of the concave sample in (b); d – Imprinted resist, on quartz, using the PDMS stamp

For the fabrication of the Al concave nanostructures we anodized 0.25 mm thick Al foil (99.999 % pure, Goodfellow) and thin Al films evaporated on supporting surfaces. For the supported samples, we used as a substrate single side polished *p*-type Si wafers (1 – 100 Ωcm, (100) crystal orientation). Prior to metal evaporation we cleaned the wafer by 15 minute sonication in acetone followed by 15 minute sonication in isopropanol and nitrogen-based drying. Metal evaporation took place in a Cryofox Explorer 600 physical vapor deposition system by subsequent e-beam evaporation of a 10 nm Ti layer (0,05 nm/s), followed by 800 nm of Al layer (0,15 nm/s). Evaporation occured under high vacuum conditions with a pressure of 3×10^{-5} mbar, while maintaing the substrates temperature at 20 °C during the evaporation. The Si wafers were hand-cut with a diamond cutter into pieces of size 25 x 25 mm^2, followed by a rinse in isopropanol and nitrogen-based drying.

Anodization of the Al samples was conducted in a home-built Teflon container, with a Brinkmann LAUDA RM 6 cooling system, under constant voltage supply by a Keithley 2400. During the anodization the temperature of the sample was maintained at a constant temperature of 0 °C for the supported samples and 5 °C for the Al foil, while the potential applied was 170 V for 10 % phosphoric acid. The anodization times for the Al foil were 51 min for the first anodization, followed by selective etching of the PAA for 6 hours, and 125 min for the second anodization following by selective etching of the PAA for 12 hours. The anodization of the evaporated Al film was 10 min followed by 1 hour PAA removal. PAA templates were etched selectively in an H_2CrO_4/H_3PO_4 mixture ($20gl^{-1}$ /70 mll^{-1}) at constant temperature of 60 °C.

The nanopatterned Al concave samples were then used as rigid masters to fabricate the PDMS stamp. For the fabrication of the PDMS stamp we used a two-part silicone elastomer Sylgard 184 (Dow Corning). The PDMS was prepared by mixing pre-polymer and curing agent in a 10 : 1 ratio and vigorous stirring. After the mixture was prepared, it was placed in a desiccator for 1 hour in order to remove any air bubbles in the mixture that were introduced by the stirring process. The Al concave masters were cleaned by sonication in acetone for 5 minutes, followed by sonication in isopropanol for 5 minutes and nitrogen-based drying. Following the cleaning process, the Al concave samples were placed in an in-house made mold by clamping the sample between two metallic plates sealed with a 20 mm in diameter and 0.2 mm thick O-ring. The thickness of the O-ring was chosen to define the thickness of the PDMS stamp. The assembly was placed in a desiccator and let to cure for 48 hours in ambient conditions according to vendor specifications. The cured PDMS stamps were peeled off from the Al concave masters in a cleanroom environment (ISO 5) to avoid contaminants residing on the PDMS surface.

For the fabrication of nanoimprinted samples, a BK7 glass wafer (500 µm thick, 100 mm diameter, double side polished, University wafers) was diced using a dicing saw (Disco DAD-2H5) into 20 mm × 15 mm sized samples. The diced samples were then cleaned following the same cleaning process as for the Si wafer mentioned earlier. Resist (AZ 5214 E from Microchemicals GmbH) was spin coated on the cleaned samples for 20 seconds at 4000 rpm. Directly after the spin coating process, the PDMS stamp

was firmly applied on the fresh photoresist, and a screw press was used to apply constant pressure onto the stamp/resist covered sample assembly during curing process on a hotplate at 140 °C for 5 minutes. After curing of the resist the PDMS stamp was peeled off from the sample and cleaned by immersing the stamp in toluene [38], rinsing with acetone followed by rinsing in isopropanol and finishing by nitrogen-based drying. In order to remove subsequently the solvents causing swelling of the PDMS stamp and reuse it, the stamp was placed on a hotplate for 1 hour at 100 °C.

For the realization of devices, metal layers were e-beam evaporated on the nanoimprinted glass samples. The cell cathodes were fabricated by evaporation of 10 nm Ti adhesive layer (0.05 nm/s), followed by 80 nm of Al (0.15 nm/s) and 8 nm of Ti (0.05 nm/s). The sample was left to for 24 hours, in order for the 8 nm Ti layer to transform into a thin TiO_x layer. Such a layer serves as a cathode interfacial layer in organic solar cells [39, 40].

The active layer was prepared from a solution of 400 mg of P3HT:PCBM (1 : 1) diluted in 10 mL of chlorobenzene and steered overnight at 600 rpm, while heated at 65 °C [40]. The active layer was then spun onto the imprinted samples in a glovebox under controlled nitrogen environment at 4000 rpm for 45 seconds and annealed at 140 °C for 5 minutes, resulting in a total film thickness of approximately 200 nm.

The fabricated Al concaves were investigated by scanning electron microscopy (SEM) (Hitachi S-4800) and reflectivity spectra were measured in a microscope setup with a 50x objective, (Nikon, model: Eclipse ME600D) using a Halogen light source and a fiber coupled spectrometer (MAYA 2000 PRO, OceanOptics), with a wavelength range from 165 nm to 1100 nm (spot size 12 μm). The morphologies of Al concaves, PDMS stamps, and imprinted concave nanopatterns were characterized by a Veeco Dimension 3100 Atomic Force Microscope (AFM) running in Tapping mode.

3. RESULTS AND DISCUSSION

In the left column in Fig. 2, 3D AFM images are shown. In (a) of a PDMS stamp fabricated after replication of Al concave patterns from Al foil, in (b) the imprinted pattern transferred on a resist covered glass sample and in (c) the imprinted pattern of the same resist covered sample in (b) directly after metal evaporation. The right column shows profile plots of the dotted black lines (left-hand side) for each AFM scan. The distance for a "hill"-to-"hill" feature (Fig. 2 a) is measured to be 438 nm, which is related to the imprinted features on the resist, measured to be 441 nm (Fig. 2 b) and the metal coated pattern measured to be 479 nm (Fig. 2 c). In addition, the width measured in the middle of each structure was measured to be 269 nm for (a), 271 nm for (b) and 280 nm for (c). Moreover, the height, measured as the distance from the highest to the lowest point, is 86.2 nm for the structures in (a), 67.8 nm for the imprinted resist in (b) and 73.6 nm for the metal covered structures in (c). These measurements indicate adequate replication of the concave patterns during the imprinting process with low rate of deformation. The deviations in the values are attributed to statistical distribution of features on the rough surfaces and the fact that we are not able to compare the same areas in the three samples throughout the replicating process.

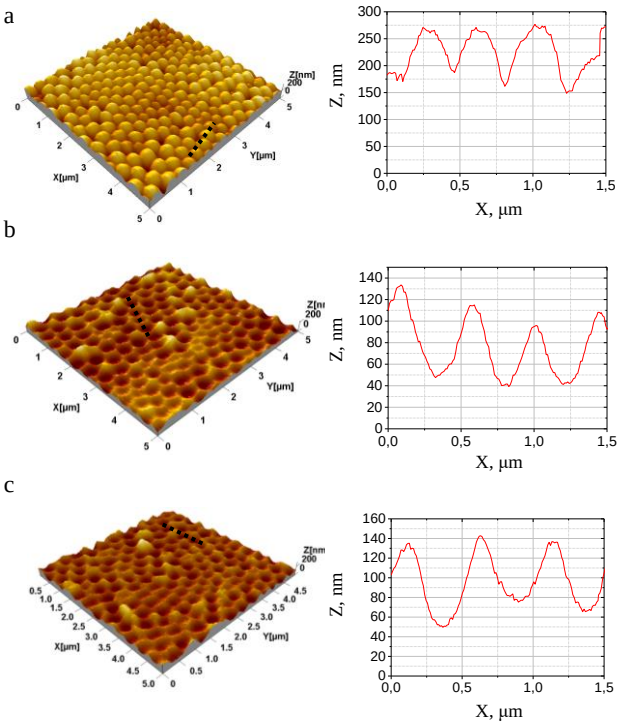

Fig. 2. Left column show 3D AFM images of: a – PDMS stamp from Al dimples (Z-range = 354 nm); b – resist imprinted quartz sample after (a) (Z-range = 223.8 nm); c – the sample in (b) after coverage with 10 nm Ti/80 nm Al/8 nm Ti metal layer (Z-rage = 285.5 nm). The right column shows the respective profiles of the black doted lines

Large concave nanostructures can easily be replicated and imprinted onto a resist surface. During anodization of Al, the formation of the PAA templates and the quality of the pores are strongly dependent on the initial Al surface [41]. On the anodization of thick Al foils this is translated to an additional step of electropolishing to create a smooth, low roughness surface for pore initialization. Without this additional step the rough surface will propagate during the anodization process, resulting in a rough underlying Al concave pattern. The effect of the surface on the microscale is shown in Fig. 3, where in (a) the red arrow points at a line irregularity in the Al concaves, which is directly transferred onto the PDMS stamp (b) fabricated from such template and therefore will end up on the imprinted resist.

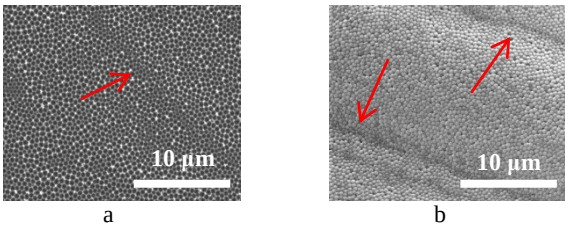

Fig. 3. SEM images of: a – Al concaves after selective removal of PAA made after anodization of Al foil in 10% H_3PO_4; b – a PDMS stamp after replication of the concave Al patterns

In addition, double anodization of Al foil is implemented to form a sacrificial PAA template during the first anodization [42] that can compensate for some irregularities on the surface. In contrast, evaporated Al films result in thin films on the substrate where surface roughness can be controlled by controlling the evaporation parameters [43, 44], resulting in films with low surface roughness. Fig. 4 a shows SEM images of Al concaves fabricated by double anodization of Al foil (no pre-treatment) where irregularities are present. Fig. 4 b shows the result for anodization of a thin Al film evaporated on Si, where due to a smooth Al film no irregularities are observed. The SEM insets in (a) and (b), show magnifications of the Al concave patterns for the Al foil and the Al thin film, respectively. It can be easily observed that the structures in (a) have a more regular honeycomb like pattern as compared to (b). This is an effect of the longer anodization process of the thick Al foil [45] as well as the two step anodization process [46].

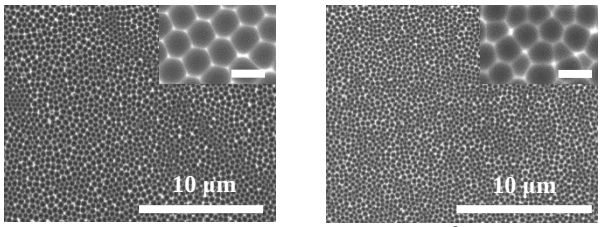

Fig. 4. SEM images of: a – Al concaves after selective removal of PAA made after anodization of Al foil in; b – Al concaves after selective removal of PAA made after anodization of thin film of Al on Si substrate. SEM insets in show zoom areas for better visualization of the ordering of the concave patterns. The scale bar in the SEM insets is 500 nm

The size of the Al concaves for the semi periodic Al concave patterns fabricated after double and long anodization of Al foil is 368 nm, while the aperiodic concave patterns fabricated after anodization of a thin Al film supported on Si result in a size of 324 nm. The deviation of the sizes of the differently fabricated Al concaves is relatively small if one takes into consideration that in order to anodize the Al foil two anodizations take place with a total time of 176 min, while the anodization of the thin Al film requires only 10 min. In addition, one should bear in mind that anodization of supported Al film results in irregularity free surface.

Fig. 5 shows 3D AFM images (left column) of the Al concave master stamp fabricated after anodization of a thin film on supporting substrate (a) and the resulting concaves with metal evaporated on top (b), after imprinting resist with a PDMS stamp. The right column shows the respective profiles of the dotted lines on the 3D AFM scans. Both surfaces show arrays of concaves with similar dimensions, denoting again that the concave patterns remain preserved throughout the imprinting process. Of importance is the height of the structures where for the Al concave master in (a) the Z-range reaches a maximum at 437.6 nm denoting that a thick organic film would be required to cover the structures in order to avoid contact of anode and cathode. in contrast, the imprinted concave pattern has a maximum Z-range of 158.8 nm, a value that is more favourable due to active layer thickness limitations in organic devices [47].

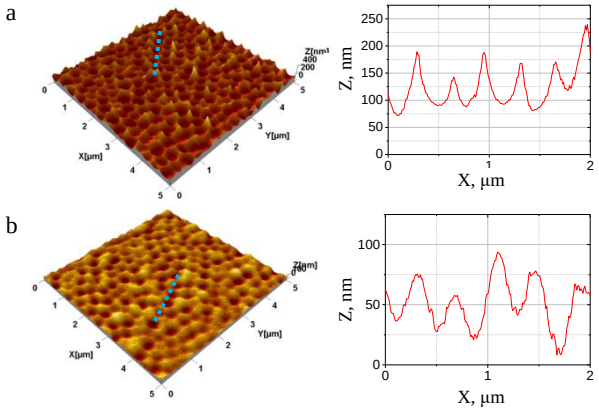

Fig. 5. Left column show 3D AFM images of: a – Al concaves on Si (Z-range = 437.6 nm); b – imprinted quartz sample after (a) (Z-rage = 158.8 nm). The sample in (b) is after coverage with 10 nm Ti/80 nm Al/8 nm Ti metal layers. The right column shows the respective profiles of the blue doted lines

The light-trapping effect of the structured surface was experimentally evaluated from reflectivity spectra of a device with non-structured metal layers on glass samples, used as a reference device, and of imprinted concave nanostructures on glass with metal layers on top. An active layer, consisting of P3HT:PCBM, was spin coated under the same parameters for both sets of devices (Fig. 6). The reflection spectrum of the reference device with planar metal layers matches with reports in the literature for P3HT:PCBM [48, 49].

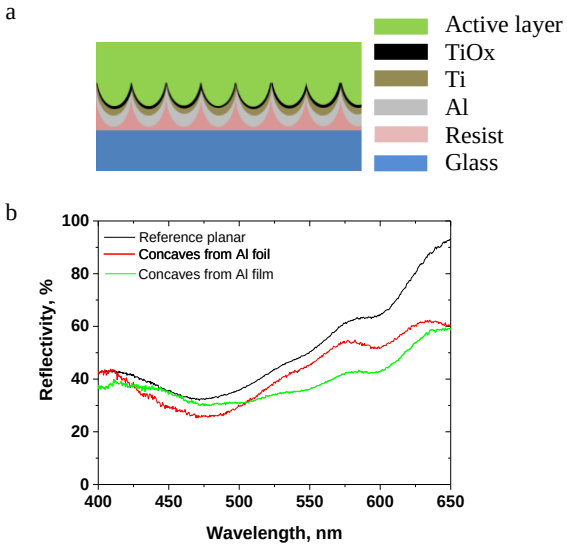

Fig. 6. a – schematics showing the device configuration for the reflectivity measurments; b – reflectivity spectra of the reference device with planar Al layer, and devices with imprinted concave patterns after replication of Al concaves from Al foil and after replication of Al concaves from thin Al film on Si substrate

The reflection spectrum of the device made from replication of Al concaves fabricated on Al foil (red curve) shows a decrease in the overall reflectivity, which corresponds to an increase in the absorption in the active layer due to the metal covered imprinted concaves. A decrease in reflectivity is also observed for devices made

from replication of Al concaves fabricated from the thin Al film (green curve). Here, a pronounced reduction in reflectivity is observed for wavelengths above 470 nm, whereas for the imprinted concaves from Al foil the reduction starts at wavelengths above 410 nm. To evaluate the accuracy of the measurements, we obtained multiple reflectivity spectra from different areas on a sample in the case of the concaves made from Al films. The uncertainty is 10 % which is clearly smaller than the presented reduction effect for wavelengths of around 500 nm and above. A similar broadband reduction effect has previously reported for larger structures acting as backside reflectors in α-Si:H solar cells, where the reduction in reflectivity of the structures has been related to diffuse scattering from the concave structures and thus related to the dimensions of the metallic nanostructures [50]. Note, however, that the overall decrease in reflectivity (and thus the increase in absorptivity) is stronger for concaves made from films as compared to concaves made from foils. The difference most probably results from the fact that the imprinted concaves from anodization of Al foil differ in dimensions and ordering from the imprinted concaves from anodization of Al thin films. This is in agreement with Tsao et al. [51]. Here, reduction in reflectance was more pronounced for structures having a more random arrangement, rather than a periodic ordering. Recently we have also shown that Al concaves can result in plasmonic field enhancements over a broad wavelength range [52], which, though, depends very sensitively on details of the actual surface morphology such as slopes and ridges. The effect of a given imprinted structure on the reflectivity spectra is thus difficult to predict.

4. CONCLUSIONS

In this work, we have presented a novel, fast method for fabrication of imprinted concave nanostructures. The nanostructures were made by anodization of (a) thick Al foils and (b) thin Al films on Si substrates in H_3PO_4 under controlled conditions, followed by selectively etching the formed porous templates. The resulting Al concave patterns were replicated via PDMS into a flexible stamp used for imprinting spin coated resist layers on glass samples.

The dimensions of the structures are similar for imprints transferred from the PDMS stamp made from semi periodic concaves from Al foil and from the PDMS stamp made from aperiodic concaves from thin Al film.

The devices with integrated metal covered imprinted concaves show a measured reduction in reflectivity denoting enhanced light absorption due to the concave patterns. The origin of the enhancement is attributed to the light trapping abilities of concave patterns presented elsewhere, and is objective of further research currently under investigation. The presented method is fast and reliable and the resulting patterns can easily be up-scaled and thus used as an alternative approach to time consuming lithographic techniques.

Acknowledgments

The research leading to these results has received funding from the People Programme (Marie Curie Actions) of the European Union's Seventh Framework Programme FP7/2007-2013/under REA Grant Agreement No. 607232. The authors thank the Mads Clausen Foundation for a research grant supporting this work. AJG would also like to thank Stefan Mátéfi-Tempfli for support on the PAA templates fabrication.

REFERENCES

1. **Tress, W.** Organic Solar Cells: Theory, Experiment, and Device Simulation *Springer* 2014: pp. 1 – 464.https://doi.org/10.1007/978-3-319-10097-5
2. **You, J., Dou, L., Zoshimura, K., Kato, T., Ohza, K., Moriarty, T., Emery, K., Chem, C.C., Gao, J., Li, G., Yang, Y.** A Polymer Tandem Solar Cell with 10.6% Power Conversion Efficiency *Nature Communications* 4 (1446) 2013: pp. 1 – 10. https://doi.org/10.1038/ncomms2411
3. **Bagher, A.M.** Introduction to Organic Solar Cells *Sustainable Energy* 2 (3) 2014: pp. 85 – 90.
4. **Cheng, Y.S., Gau, C.** Efficiency Improvement of Organic Solar Cells with Imprint of Nanostructures by Capillary Force Lithography *Solar Energy Materials and Solar Cells* 120 2014: pp. 566 – 571.
5. **Wiedemann, W., Sims, L., Abdellah, A., Exner, A., Meier, R., Musselman, K.P., MacManus-Driscoll, J.L., Müller-Buschbaum, P., Scarpa, G., Lugli, P., Schmidt-Mende, L.** Nanostructured Interfaces in Polymer Solar Cells *Applied Physics Letters* 96 (26) 2010: pp. 263109-1 – 263109-3.
6. **Ray, B., Khan, M.R., Black, C., Alam, M.A.** Nanostructured Electrodes for Organic Solar Cells : Analysis and Design Fundamentals *IEEE Journal of Photovoltaics* 3 (1) 2013: pp. 318 – 329. https://doi.org/10.1109/JPHOTOV.2012.2220529
7. **Tang, Z., Tress, W., Inganäs, O.** Light Trapping in Thin Film Organic Solar Cells *Materials Today* 17 (8) 2014: pp. 389 – 396.
8. **Chou, C.H., Chen, F.C.** Plasmonic Nanostructures for Light Trapping in Organic Photovoltaic Devices *Nanoscale* 6 (15) 2014: pp. 8444 – 8458.
9. **Yun, J., Wang, W., Kim, S.M., Bae, T.S., Lee, S., Kim, D., Lee, G.H., Lee, H.S., Song, M.** Light Trapping in Bendable Organic Solar Cells Using Silica Nanoparticle Arrays *Energy Environmental Science* 8 (3) 2015: pp. 932 – 940.
10. **Cho, C., Kim, H., Jeong, S., Baek, S.W., Seo, J.W., Han, D., Kim, K., Park, Y., Yoo, S., Lee, J.Y.** Random and V-Groove Texturing for Efficient Light Trapping in Organic Photovoltaic Cells *Solar Energy Materials and Solar Cells* 115 2013: pp. 36 – 41.
11. **de Oliveira Hansen, R.M., Liu, Y., Madsen, M., Rubahn, H.G.** Flexible PCPDTBT:PCBM Solar Cells with Integrated Grating Structures *SPIE Organic Photovoltaics XIV 8830* 2013: pp. 883021-1 – 883021-7.
12. **Li, X.H., Sha, W.E.I., Choy, W.C.H., Fung, D.D.S., Xie, F.X.** Efficient Inverted Polymer Solar Cells with Directly Patterned Active Layer and Silver Back Grating *The Journal of Physical Chemistry C* 116 (12) 2012: pp. 7200 – 7206.
13. **Na, S.I., Kim, S.S., Jo, J., Oh, S.H., Kim, J., Kim, D.Y.** Efficient Polymer Solar Cells with Surface Relief Gratings Fabricated by Simple Soft Lithography *Advanced Functional Materials* 18 (24) 2008: pp. 3956 – 3963.
14. **Catchpole, K.R., Polman, A.** Plasmonic Solar Cells *Optics Express* 16 (26) 2008: pp. 21793 – 21800. https://doi.org/10.1364/OE.16.021793
15. **Ferry, V.E., Munday, J.N., Atwater, H.A.** Design Considerations for Plasmonic Photovoltaics *Advanced Materials* 22 (43) 2010: pp. 4794 – 808.
16. **Duche, D., Torchio, P., Escoubas, L., Monestier, F., Simon, J.J., Flory, F., Mathian, G.** Improving Light Absorption in Organic Solar Cells by Plasmonic Contribution *Solar Energy Materials and Solar Cells* 93 (8) 2009: pp. 1377 – 1382. https://doi.org/10.1016/j.solmat.2009.02.028
17. **Baek, S.W., Noh, J., Lee, C.H., Kim, B.S., Seo, M.K., Lee, J.Y.** Plasmonic Forward Scattering Effect in Organic Solar Cells: A Powerful Optical Engineering Method *Scientific Reports* 3 (1726) 2013: pp. 1 – 7.
18. **Guo, L.J.** Nanoimprint Lithography: Methods and Material Requirements *Advanced Materials* 19 (4) 2007: pp. 495 – 513.
19. **Zhou, W.** Nanoimprint Lithography: An Enabling Process for

Nanofabrication, *Springer*, 2013: pp. 1 – 146. https://doi.org/10.1007/978-3-642-34428-2_1

20. **Kang, M.G., Kim, M.S., Kim, J., Guo, L.J.** Organic Solar Cells Using Nanoimprinted Transparent Metal Electrodes *Advanced Materials* 20 (23) 2008: pp. 4408 – 4413. https://doi.org/10.1002/adma.200800750
21. **Wang, D.H., Choi, D.G., Lee, K.J., Jeong, J.H., Jeon, S.H., Park, O.O., Park, J.H.** Effect of the Ordered 2D-dot Nano-patterned Anode for Polymer Solar Cells *Organic Electronics* 11 (2) 2010: pp. 285 – 290.
22. **Chen, B.C., Cheng, Y.S., Gau, C., Lee, Y.C.** Enhanced Performance of Polymer Solar Cells with Imprinted Nanostructures on the Active Layer *Thin Solid Films* 564 2014: pp. 384 – 389.
23. **Lee, K., Tang, Y., Ouyang, M.** Self-ordered, Controlled Structure Nanoporous Membranes using Constant Current Anodization *Nano Letters* 8 (12) 2008: pp. 4624 – 4629. https://doi.org/10.1021/nl803271c
24. **Diggle, J.W., Downie, T.C., Goulding, C.W.** Anodic Oxide Films on Aluminum *Chemical Reviews* 69 (3) 1969: pp. 365 – 405.
25. **Lee, W., Park, S.J.** Porous Anodic Aluminum Oxide: Anodization and Templated Synthesis of Functional Nanostructures *Chemical Reviews* 114 (15) 2014: pp. 7487 – 7556.
26. **Wu, H., Yang, J., Cao, S., Huang, L., Chen, L.** Ordered Organic Nanostructures Fabricated from Anodic Alumina Oxide Templates for Organic Bulk-Heterojunction Photovoltaics *Macromolecular Chemistry and Physics* 215 (7) 2014: pp. 584 – 596. https://doi.org/10.1002/macp.201300766
27. **Lee, J.H., Kim, D.W., Jang, H., Choi, J.K., Geng, J., Jung, J.W., Yoon, S.C., Jung, H.T.** Enhanced Solar-cell Efficiency in Bulk-heterojunction Polymer Systems Obtained by Nanoimprinting with Commercially Available AAO Membrane Filters *Small* 5 (19) 2009: pp. 2139 – 2143.
28. **Aryal, M., Buyyukserin, F., Mielczarek, K., Zhao, X.M., Gao, J., Zakhidov, A., Hu, W.W.** Imprinted Large-scale High Density Polymer Nanopillars for Organic Solar Cells *Journal of Vacuum Science & Technology B: Microelectronics and Nanometer Structures* 26 (6) 2008: pp. 2562 – 2566.
29. **Hu, J., Shirai, Y., Han, L., Wakayama, Y.** Template Method for Fabricating Interdigitate p-n Heterojunction for Organic Solar Cell *Nanoscale research letters* 7 (469) 2012: pp. 1 – 5.
30. **Dunbar, R.B., Pfadler, T., Lal, N.N., Baumberg, J.J., Schmidt-Mende, L.** Imprinting Localized Plasmons for Enhanced Solar Cells *Nanotechnology* 23 (385202) 2012: pp. 1 – 5.
31. **Ono, S., Saito, M., Asoh, H.** Self-ordering of Anodic Porous Alumina Formed in Organic Acid Electrolytes *Electrochimica Acta* 51 (5) 2005: pp. 827 – 833.
32. **Norek, M., Dopierała, M., Stępniowski, W.J.** Ethanol Influence on Arrangement and Geometrical Parameters of Aluminum Concaves Prepared in a Modified Hard Anodization for Fabrication of Highly Ordered Nanoporous Alumina *Journal of Electroanalytical Chemistry* 750 2015: pp. 79 – 88.
33. **Norek, M., Włodarski, M., Stępniowski, W.J.** Tailoring of UV/violet Plasmonic Properties in Ag, and Cu Coated Al Concaves Arrays *Applied Surface Science* 314 2014: pp. 807 – 814.
34. **Md Jani, A.M., Losic, D., Voelcker, N.H.** Nanoporous Anodic Aluminium Oxide: Advances in Surface Engineering and Emerging Applications *Progress in Materials Science* 58 (5) 2013: pp. 636 – 704.
35. **Poinern, G.E.J., Ali, N., Fawcett, D.** Progress in Nano-Engineered Anodic Aluminum Oxide Membrane Development *Materials* 4 (3) 2010: pp. 487 – 526.
36. **Lee, W., Nielsch, K., Gösele, U.** Self-Ordering Behavior of Nanoporous Anodic Aluminum Oxide (AAO) in Malonic Acid Anodization *Nanotechnology* 18 (47) 2007: pp. 475713-1 – 475713-8.
37. **Zaraska, L., Kurowska, E., Sulka, G.D., Senyk, I., Jaskula, M.** The Effect of Anode Surface Area on Nanoporous Oxide Formation During Anodizing of Low Purity Aluminum (AA1050 alloy) *Journal of Solid State Electrochemistry* 18 (2) 2013: pp. 361 – 368. https://doi.org/10.1007/s10008-013-2215-z
38. **Lee, J.N., Park, C., Whitesides, G.M.** Solvent Compatibility of Poly(dimethylsiloxane)-Based Microfluidic Devices *Analytical Chemistry* 75 (23) 2003: pp. 6544 – 6554.
39. **Waldauf, C., Morana, M., Denm, P., Schilinsky, P., Coakley, K., Choulis, S.A., Brabec, C.J.** Highly Efficient Inverted Organic Photovoltaics Using Solution Based Titanium Oxide as Electron Selective Contact *Applied Physics Letters* 89 (23) 2006: pp. 233517-1 – 233517-3.
40. **de Oliveira Hansen, R.M., Liu, Y., Madsen, M., Rubahn, H.G.** Flexible Organic Solar Cells Including Efficiency Enhancing Grating Structures *Nanotechnology* 24 (14) 2013: pp. 145301-1 – 145301-6.
41. **Yu, C.U., Hu, C.C., Bai, A., Yang, Y.F.** Pore-Size Dependence of AAO Films on Ssurface Roughness of Al-1050 Sheets Controlled by Electropolishing Coupled with Fractional Design *Surface and Coatings Technology* 201 (16 – 17) 2007: pp. 7259 – 7265.
42. **Ferré-Borrull, J., Pallarès, J., Macías, G., Marsal, L.** Nanostructural Engineering of Nanoporous Anodic Alumina for Biosensing Applications *Materials* 7 (7) 2014: pp. 5225 – 5253.
43. **Bordo, K., Rubahn, H.G.** Effect of Deposition Rate on Structure and Surface Morphology of Thin Evaporated Al Films on Dielectrics and Semiconductors *Materials Science* 18 (4) 2012: pp. 313 – 317.
44. **Ottone, C., Laurenti, M., Bejtka, K., Sangrinario, A., Cauda, V.** The Effects of the Film Thickness and Roughness in the Anodization Process of Very Thin Aluminum Films *Journal of Materials Science & Nanotechnology* 1 (1) 2014: pp. 1 – 9.
45. **Surawathanawises, K., Cheng, X.** Nanoporous Anodic Aluminum Oxide with a Long-Range Order and Tunable Cell Sizes by Phosphoric Acid Anodization on Pre-Patterned Substrates *Electrochimica acta* 117 2014: pp. 498 – 503. https://doi.org/10.1016/j.electacta.2013.11.144
46. **Masuda, H., Fukuda, K.** Ordered Metal Nanohole Arrays Made by a Two-Step Replication of Honeycomb Structures of Anodic Alumina *Science* 268 (5216) 1995: pp. 1466 – 1468.
47. **Leung, S.F., Zhang, Q., Xiu, F., Yu, D., Ho, J.C., Li, D., Fan, Z.** Light Management with Nanostructures for Optoelectronic Devices *The journal of physical chemistry letters* 5 (8) 2014: pp. 1479 – 1495.
48. **Cook, S., Katoh, R., Furube, A.** Ultrafast Studies of Charge Generation in PCBM:P3HT Blend Films following Excitation of the Fullerene PCBM *The Journal of Physical Chemistry C* 113(6) 2009: pp. 2547 – 2552. https://doi.org/10.1021/jp8050774
49. **Shrotriya, V., Ouyang, J., Tseng, R.J., Li, G., Yang, Y.** Absorption Spectra Modification in poly(3-hexylthiophene):methanofullerene Blend Thin Films *Chemical Physics Letters* 411 (1 – 3) 2005: pp. 138 – 143.
50. **Tsao, Y.C., Sødergaard, T., Kristensen, P.K., Rizzoli, R., Pedersen, K., Pedersen, T.G.** Rapid Fabrication and Trimming of Nanostructured Backside Reflectors for Enhanced Optical Absorption in a-Si:H Solar Cells *Applied Physics A* 120 (2) 2015: pp. 417 – 425. https://doi.org/10.1007/s00339-015-9205-1
51. **Tsao, Y.C. Sødergaard, T., Skovsen, E., Gurevich, L., Pedersen, K., Pedersen, T.G.** Pore Size Dependence of Diffuse Light Scattering from Anodized Aluminum Solar Cell Backside Reflectors *Optics express* 21 (S1) 2013: pp. A84 – A95.
52. **Goszczak, A.J., Adam, J., Cielecki, P.P., Fiutowski, J., Rubahn, H.G., Madsen, M.** Nanoscale Aluminum Concaves for Light-Trapping in Organic Thin Films *Optics Communications* 370 2016: pp. 135-139.